Inorganic Chemistry

Article

pubs.acs.org/IC

Lead(II) Complex Formation with L-Cysteine in Aqueous Solution

Farideh Jalilehvand,*[,†] Natalie S. Sisombath,[†] Adam C. Schell,[†] and Glenn A. Facey[‡]

[†]Department of Chemistry, University of Calgary, 2500 University Drive NW, Calgary, Alberta T2N 1N4, Canada

[‡]Department of Chemistry, University of Ottawa, 10 Marie Curie Private, Ottawa, Ontario K1N 6N5, Canada

Supporting Information

ABSTRACT: The lead(II) complexes formed with the multidentate chelator L-cysteine (H_2Cys) in an alkaline aqueous solution were studied using ^{207}Pb, ^{13}C, and ^{1}H NMR, Pb L_{III}-edge X-ray absorption, and UV−vis spectroscopic techniques, complemented by electrospray ion mass spectrometry (ESI-MS). The H_2Cys/Pb^{II} mole ratios were varied from 2.1 to 10.0 for two sets of solutions with $C_{Pb^{II}}$ = 0.01 and 0.1 M, respectively, prepared at pH values (9.1−10.4) for which precipitates of lead(II) cysteine dissolved. At low H_2Cys/Pb^{II} mole ratios (2.1−3.0), a mixture of the dithiolate $[Pb(S,N\text{-}Cys)_2]^{2-}$ and $[Pb(S,N,O\text{-}Cys)(S\text{-}HCys)]^{-}$ complexes with average Pb−(N/O) and Pb−S distances of 2.42 ± 0.04 and 2.64 ± 0.04 Å, respectively, was found to dominate. At high concentration of free cysteinate (>0.7 M), a significant amount converts to the trithiolate $[Pb(S,N\text{-}Cys)(S\text{-}HCys)_2]^{2-}$, including a minor amount of a PbS_3-coordinated $[Pb(S\text{-}HCys)_3]^{-}$ complex. The coordination mode was evaluated by fitting linear combinations of EXAFS oscillations to the experimental spectra and by examining the ^{207}Pb NMR signals in the chemical shift range δ_{Pb} = 2006−2507 ppm, which became increasingly deshielded with increasing free cysteinate concentration. One-pulse magic-angle-spinning (MAS) ^{207}Pb NMR spectra of crystalline $Pb(aet)_2$ (Haet = 2-aminoethanethiol or cysteamine) with PbS_2N_2 coordination were measured for comparison (δ_{iso} = 2105 ppm). The UV−vis spectra displayed absorption maxima at 298−300 nm ($S^- \rightarrow Pb^{II}$ charge transfer) for the dithiolate $PbS_2N(N/O)$ species; with increasing ligand excess, a shoulder appeared at ∼330 nm for the trithiolate PbS_3N and PbS_3 (minor) complexes. The results provide spectroscopic fingerprints for structural models for lead(II) coordination modes to proteins and enzymes.

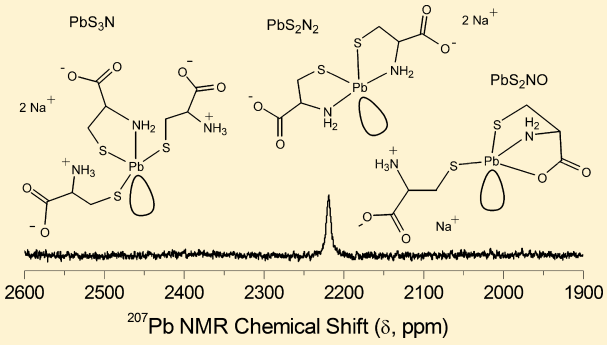

INTRODUCTION

The efficiency of cysteine-rich proteins and peptides, e.g., metallothioneins and phytochelatins, in removing harmful heavy metals from the cells and tissues[1,2] has inspired the assessment of cysteine as an ecofriendly agent for extracting heavy metals from a contaminated environment. Cysteine (H_2Cys = $HSCH_2CH(NH_3^+)COO^-$), as well as penicillamine (H_2Pen) and glutathione (GSH), can liberate lead bound in contaminated soil, in iron/manganese oxides, and in lead phosphate/carbonate salts or in mine tailings by increasing its solubility and mobilization.[3−5] Moreover, the ability of cysteine to capture heavy metals including lead from polluted water can be important in the development of new materials with potential use in drainage and wastewater treatment.[6] A cysteine-based nanosized chelating agent that selectively removes Pb^{II} ions has recently been developed for the treatment of lead poisoning.[7]

In recent years, cysteine has been introduced as an environmentally friendly source of sulfur for preparing nanocrystalline PbS, a widely used semiconductor. Such nanocrystals can be prepared by mixing $Pb(NO_3)_2$ or $Pb(OAc)_2$ (OAc^- = acetate) with cysteine to form a lead(II) cysteine precursor, followed by hydrothermal decomposition to PbS. Different morphologies, shapes, and sizes can be obtained depending on the metal-to-ligand mole ratio, concentration, or pH.[8−11] It has been suggested that the precursor is polycrystalline $HSCH_2CH(NH_2)COOPbOH$[8] or has a polymeric $[-SCH_2CH(COOH)NHPb-]_n$ structure,[11] in well-aligned one-dimensional nanowires.[12]

Corrie and co-workers have reported formation constants for several mononuclear lead(II) cysteine complexes in aqueous solution, including Pb(Cys), $Pb(Cys)_2^{2-}$, $Pb(Cys)_3^{4-}$, $Pb(HCys)^+$, $Pb(Cys)(HCys)^-$, and $Pb(Cys)_2(OH)^{3-}$, however, with revised values, e.g., for the Pb(Cys) complex in their later reports.[13−15] Bizri and co-workers also reported formation constants for the above complexes, except for $Pb(Cys)_3^{4-}$ and $Pb(Cys)_2(OH)^{3-}$, but included a $Pb(Cys)(OH)^-$ complex; see Figure S-1a in the Supporting Information (SI).[16] To explain the high stability of the Pb(Cys) complex, cysteinate was proposed to act as a tridentate ligand, binding simultaneously through the thiolate ($-S^-$), carboxylate ($-COO^-$), and amine ($-NH_2$) groups.[15−17] However, a subsequent study of the COO^- stretching frequencies indicated that cysteinate in an alkaline solution exclusively binds to Pb^{II} via the amine and thiolate groups.[18] Pardo et al. proposed formation constants for

Received: October 22, 2014
Published: February 19, 2015

DOI: 10.1021/ic5025668
Inorg. Chem. 2015, 54, 2160−2170

a set consisting of the Pb(Cys), $Pb(HCys)^+$, $Pb(HCys)_2$, $Pb(Cys)(HCys)^-$, and $Pb(Cys)_2^{2-}$ complexes.[19] Recently, Crea et al. obtained formation constants for Pb(Cys), $Pb(HCys)^+$, $Pb(H_2Cys)^{2+}$, $Pb(Cys)(OH)^-$, and $Pb(Cys)_2^{2-}$ to describe the stoichiometric composition of the lead(II) cysteine complexes formed at several ionic strengths ($0 < I \leq 1.0$ M $NaNO_3$) and temperatures; see Figure S-2a in the SI.[20] The highest Pb^{II} concentration used in all studies above was 0.5 mM.

In a high-field ^1H and ^{13}C NMR study, Kane-Maguire and Riley investigated the Pb^{II} binding to cysteine at both acidic (pD 1.9) and alkaline (pD 12.9) D_2O solutions.[21] The report includes proton-coupling constants for free cysteine (L), as well as mole fractions of its three rotamers: trans (*t*) and gauche (*g* and *h*), at different pD values in the range 1.80−12.92 (pD = pH reading + 0.4).[21,22] Each rotamer was ascribed a preferred mode of binding: rotamer *t* to bidentate (*S,N*), *h* to tridentate (*S, N, O*), and *g* to bidentate (*S,O*). No significant lead(II) cysteine complex formation was observed in the acidic solutions (pD 1.9) with H_2Cys/Pb^{II} mole ratios 0.5−6.0, which is consistent with the well-known ability of lead(II) to form nitrate complexes.[23] At $H_2Cys/Pb(NO_3)_2$ mole ratios ≥2.0 ($C_{Pb^{II}}$ = 10 mM), only PbL_2 complexes were proposed to form in alkaline media (pD 12.9), with cysteine mainly acting as a tridentate (*S,N,O*) or a bidentate (*S,N*) ligand. It was also suggested that when $C_{Pb(NO_3)_2} = C_{H_2Cys}$ = 10 mM (pD 12.9), PbL species with 63% Pb(*S,N,O*-Cys), 30% Pb(*S,O*-Cys), and 7% Pb(*S,N*-Cys) coordination were formed in proportion to the mole fractions of *h*, *g*, and *t* rotamers, respectively. However, we could not prepare aqueous solutions with 1:1 Pb^{II}/cysteine composition because the initially formed precipitate did not dissolve in alkaline media even at pH 12.0, and stability constants for lead(II) hydrolysis indicate that precipitation of lead(II) hydroxide should start in such highly alkaline media;[20] see Figures S-1b and S-2b in the SI.

Reliable structural information to allow a better understanding of the nature of the lead(II) complexes formed with cysteine is clearly needed. We used a combination of spectroscopic techniques, including UV−vis, ^{207}Pb, ^{13}C, and ^1H NMR, extended X-ray absorption fine structure (EXAFS), and electrospray ion mass spectrometry (ESI-MS) to study the coordination and bonding in lead(II) cysteine complexes formed in two sets of alkaline solutions with $C_{Pb^{II}}$ = 10 and 100 mM for H_2Cys/Pb^{II} mole ratios ≥2.1. To obtain such concentrations, the pH was raised (9.1−10.4) to dissolve the lead(II) cysteine precipitate that forms when adding lead(II) to cysteine solutions. Both the −SH and $-NH_3^+$ groups of cysteine deprotonate at about pH 8.5,[24] thus increasing its ability to coordinate via the thiolate and amine groups.

EXPERIMENTAL SECTION

Sample Preparation. L-Cysteine, cysteamine (Haet, $H_2NCH_2CH_2SH$), PbO, $Pb(ClO_4)_2{\cdot}3H_2O$, and sodium hydroxide were used as supplied (Sigma-Aldrich). All syntheses were carried out under a stream of argon gas. Deoxygenated water for sample preparation was prepared by bubbling argon gas through boiled distilled water. The pH values of the solutions were monitored with a Thermo Scientific Orion Star pH meter.

Two sets of lead(II) cysteine solutions were prepared with different $H_2Cys/Pb(ClO_4)_2$ mole ratios for $C_{Pb^{II}} \sim 10$ and 100 mM, respectively, at an alkaline pH at which the lead(II) cysteine precipitate dissolved; see Table 1. Lead(II) cysteine solutions A−G ($C_{Pb^{II}} \approx 10$ mM) and A*−F* ($C_{Pb^{II}} \approx 100$ mM) were freshly prepared by adding $Pb(ClO_4)_2{\cdot}3H_2O$ (0.05 mmol) to cysteine dissolved in deoxygenated water (0.105−0.75 mmol, pH 2.0−2.4). For ^{207}Pb NMR and UV−vis measurements of solutions A−G, 50 mM stock solutions of enriched ^{207}PbO (94.5%) from Cambridge Isotope Laboratories and PbO dissolved in 0.15 M $HClO_4$ were prepared, respectively. Upon the dropwise addition of 6.0 M NaOH, an off-white precipitate formed, which momentarily dissolved at pH ∼7; after a few seconds, a cream-colored precipitate appeared. The addition of a 1.0 M sodium hydroxide solution continued until the solid dissolved above pH 8.5 and gave a clear colorless solution. For solutions A ($C_{Pb^{II}}$ = 10 mM) and A* ($C_{Pb^{II}}$ = 100 mM), with the mole ratio H_2Cys/Pb^{II} = 2.1, the solid dissolved completely at pH ∼10.4, and for solutions B and B* (H_2Cys/Pb^{II} mole ratio = 3.0), it dissolved at pH 9.1. For consistency, the pH values of solutions with higher H_2Cys/Pb^{II} mole ratios were also set at pH 9.1. The final volume for each solution was adjusted to 5.0 mL. Solutions A−F were used for ESI-MS and ^1H and ^{13}C NMR (prepared in 99.9% deoxygenated D_2O) measurements. For solutions in D_2O, the pH-meter reading was 10.4 for solution A (pD = pH reading + 0.4)[22] and 9.1 for B−F. ^{207}Pb NMR spectra were measured for all solutions (10% v/v D_2O), while Pb L_{III}-edge EXAFS spectra were measured for solutions A−E and A*−F*.

Table 1. Composition of Lead(II) Cysteine Solutions

H_2Cys/Pb^{II} mole ratio	pH	solution	$C_{Pb^{II}}$ (mM)	solution	$C_{Pb^{II}}$ (mM)
2.1	10.4	A	10	A*	100
3.0	9.1	B	10	B*	100
4.0	9.1	C	10	C*	100
5.0	9.1	D	10	D*	100
8.0	9.1	E	10	E*	100
10.0	9.1	F	10	F*	100
15.0	9.1	G	10		
15.0	8.9	G′	10		

Bis(2-aminoethanethiolato)lead(II) Solid, Pb(aet)$_2$. A total of 0.964 g (12.5 mmol) of Haet dissolved in 10 mL of deoxygenated water (pH 9.6) was added to a suspension of PbO (1.116 g, 5 mmol) in 50 mL of ethanol at 50 °C and refluxed for 3 h under an argon atmosphere, giving a pale-yellow solution, which was then filtered and cooled in a refrigerator. Colorless crystals formed after 48 h and were filtered, washed with ethanol, and dried under vacuum (turning yellow). Eleme anal. Calcd for $Pb(SCH_2CH_2NH_2)_2$: C, 13.36; H, 3.37; N, 7.79. Found: C, 13.41; H, 3.43; N, 7.81. The unit cell dimensions of the crystal were also verified, matching the literature values.[25]

Methods. Details about instrumentation and related procedures for ESI-MS (Aglient 6520 Q-Tof), UV−vis (Cary 300), and ^1H, ^{13}C, and ^{207}Pb NMR spectroscopy (Bruker AMX 300 and Avance II 400 MHz), as well as EXAFS data collection and data analyses are provided elsewhere.[26] UV−vis spectra of solutions A−G were measured using 0.25, 0.5, and 0.75 nm data intervals, with a 1.5 absorbance Agilent rear-beam attenuator mesh filter in the reference position. ESI-MS spectra for solutions A, B, and F were measured in both positive- and negative-ion modes. ^{207}Pb NMR spectra for solutions A−G enriched in ^{207}Pb were measured at room temperature using a Bruker AMX 300 equipped with a 10 mm broad-band probe. For these solutions, the ^{207}Pb NMR chemical shift was externally calibrated relative to 1.0 M $Pb(NO_3)_2$ in D_2O, resonating at −2961.2 ppm relative to $Pb(CH_3)_4$ (δ = 0 ppm).[27] Approximately 12800−51200 scans for ^{207}Pb NMR, 16−32 scans for ^1H NMR, and 500−3000 scans for ^{13}C NMR were coadded for the solutions. One-pulse magic-angle-spinning (MAS) ^{207}Pb NMR spectra for crystalline $Pb(aet)_2$ were acquired with high-power proton decoupling on an AVANCE III 200 NMR spectrometer at room temperature (^{207}Pb, 41.94 MHz). Ground crystals were packed in a 7 mm zirconia rotor, spinning at MAS rates of 5.8 and 5.5 kHz using 800 and 895 scans, respectively, with a 5.0 s recycle delay. Chemical shifts were referenced relative to $Pb(CH_3)_4$, by setting the ^{207}Pb NMR peak of solid $Pb(NO_3)_2$ spinning at a 1.7 kHz rate at −3507.6 ppm (295.8 K).[28,29] Static ^{207}Pb NMR powder patterns were reconstructed by iteratively fitting the sideband manifold using the *Solids Analysis* package within Bruker's *TOPSPIN 3.2* software.

DOI: 10.1021/ic5025668
Inorg. Chem. 2015, 54, 2160−2170

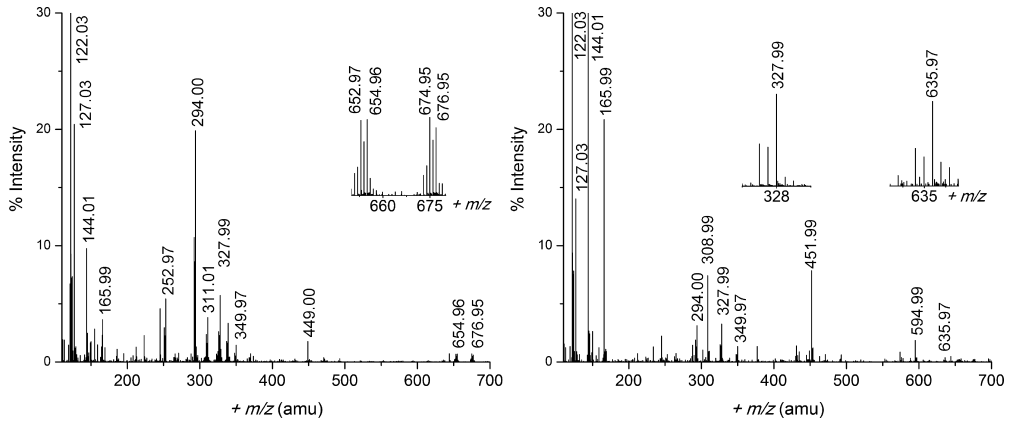

Figure 1. ESI-MS spectra measured in positive-ion mode for solutions A (left) and F (right) ($C_{Pb^{II}}$ = 10 mM) with H_2Cys/Pb^{II} mole ratios 2.1 and 10.0, respectively. The peak at 122.03 amu has 100% intensity. Selected peaks assigned to lead(II) species with distinct isotopic patterns for Pb are shown in the inset.

Pb L_{III}-edge X-ray absorption spectroscopy (XAS) spectra were measured at ambient temperature at the Stanford Synchrotron Radiation Lightsource (SSRL) for freshly prepared solutions A–E and A* at BL 7-3 (500 mA; equipped with a rhodium-coated harmonic rejection mirror) and for solutions B*–F* at BL 2-3 (100 mA). A double-crystal monochromator with Si(220) was used at both beamlines. To remove higher harmonics, the monochromator was detuned to eliminate 50% of the maximum intensity of the incident beam (I_0) at the end of the scan at BL 2-3. To avoid photoreduction of the samples at BL 7-3, the beam size was adjusted to 1 × 1 mm, and the intensity of the incident beam was reduced to 80% of the maximum of I_0 at 13806 eV. A high beam intensity could result in precipitation of a small amount of black particles in the sample holder, especially in solutions containing excess ligand. For solutions containing $C_{Pb^{II}}$ = 10 mM, 12–13 scans were measured in both transmission and fluorescence modes, detecting X-ray fluorescence using a 30-channel germanium detector, while for the more concentrated solutions with $C_{Pb^{II}}$ = 100 mM between three and four scans were collected in transmission mode. For each sample, consecutive scans were averaged after comparison to ensure that no radiation damage had occurred. The energy scale was internally calibrated by assigning the first inflection point of a lead foil at 13035.0 eV. The threshold energy E_0 in the XAS spectra of the lead(II) cysteine solutions varied within a narrow range: 13034.0–13034.9 eV. Least-squares curve fitting of the EXAFS spectra was performed for solutions A, B, A*, B*, and F* over the k range = 2.7–11.7 $Å^{-1}$, using the D-penicillaminatolead(II) (PbPen) crystal structure[30] as the model in the *FEFF 7.0* program.[31,32] For each scattering path, the refined structural parameters were the bond distance (R), the Debye–Waller parameter (σ^2), and in some cases the coordination number (N). The amplitude reduction factor (S_0^2) was fixed at 0.9 (obtained from EXAFS data analysis of solid PbPen),[33] while ΔE_0 was refined as a common value for all scattering paths. The accuracy of the Pb–(N/O) and Pb–S bond distances and the corresponding Debye–Waller parameters is within ±0.04 Å and ±0.002 $Å^2$, respectively. Further technical details about EXAFS data collection and data analyses were provided previously.[26]

Principal component analysis (PCA), introduced in the *EXAFSPAK* suite of programs,[34] was applied on the raw k^3-weighted experimental EXAFS spectra for solutions A–E and A*–F* over the k range of 2.7–11.7 $Å^{-1}$. *DATFIT*, another program in the *EXAFSPAK* package, was used to fit the k^3-weighted EXAFS spectra of lead(II) cysteine solutions A–E and A*–F* to a linear combination of EXAFS oscillations for species with $PbS_2N(N/O)$, PbS_3N, and PbS_3 coordination to estimate the amount of such species in each lead(II) cysteine solution. For the PbS_3N model, theoretical EXAFS oscillations were simulated by stepwise variation of the Pb–S and Pb–N parameters: Pb–S 2.67–2.70 Å [using σ^2 = 0.0065 $Å^2$ from EXAFS least-squares refinement of lead(II) glutathione solutions with excess ligand],[33] Pb–N 2.40–2.43 Å (σ^2 = 0.004, 0.006, and 0.008 $Å^2$), and S_0^2 = 0.9. The best fits were obtained for Pb–S = 2.68 Å (σ^2 = 0.0065 $Å^2$) and Pb–N = 2.40 Å (σ^2 = 0.0080 $Å^2$).

RESULTS

ESI-MS. ESI-MS spectra were measured in both positive- and negative-ion modes for the lead(II) cysteine solutions A, B, and F, with $C_{Pb^{II}}$ = 10 mM and H_2Cys/Pb^{II} mole ratios 2.1, 3.0, and 10.0, respectively, as shown in Figures 1 and S-3 in the SI, to identify possible charged lead(II) cysteine complexes. The assignment of the mass ions, presented in Tables 2 and S-1 in the SI, is facilitated by the distinct isotopic distribution pattern for lead(II) species due to the natural abundance of 52.4% ^{208}Pb, 22.1% ^{207}Pb, 24.1% ^{206}Pb, and 1.4% ^{204}Pb.[35] The ESI-MS spectra for solutions A and B were nearly identical, showing positive-ion mass peaks for species with metal-to-ligand mole ratios 1:1, 1:2, and 2:2. Such mass peaks were also previously detected for a 1:1 mixture of $Pb(NO_3)_2$ and cysteine in 50% methanol/water and considered to be independent of the reaction mixture stoichiometry (1:10 or 10:1).[36] We could also detect a 1:3 species $[3Na^+ + Pb(H_2Cys)_3 - 4H^+]^+$ at 635.97

Table 2. Assignment of Mass Ions Observed in ESI-MS Spectra (Positive-Ion Mode) for Lead(II) Cysteine Solutions A, B, and F ($C_{Pb^{II}}$ = 10 mM; H_2Cys/Pb^{II} Mole Ratios 2.1, 3.0, and 10.0, Respectively)[a]

m/z (amu)	assignment	m/z (amu)	assignment
122.03	$[H_2Cys + H^+]^+$	327.99	$[Pb(H_2Cys) - H^+]^+$
144.01	$[Na^+ + H_2Cys]^+$	349.97	$[Na^+ + Pb(H_2Cys) - 2H^+]^+$
165.99	$[2Na^+ + H_2Cys - H^+]^+$	449.00	$[Pb(H_2Cys)_2 - H^+]^+$
252.97	$[Pb(HCOO)]^+$	451.99	$[4Na^+ + 3(H_2Cys) - 3H^+]^+$
294.00	$[Pb(H_2Cys) - H^+ - H_2S]^+$	594.99	$[5Na^+ + 4(H_2Cys) - 4H^+]^+$
308.99	$[3Na^+ + 2(H_2Cys) - 2H^+]^+$	635.97	$[3Na^+ + Pb(H_2Cys)_3 - 4H^+]^+$
311.01	$[PbC_2H_5N_3O_2]^+$	654.96	$[Pb_2(H_2Cys)_2 - 3H^+]^+$
		676.95	$[Na^+ + Pb_2(H_2Cys)_2 - 4H^+]^+$

[a] H_2Cys ($C_3H_7NO_2S$); m/z 121.02.

DOI: 10.1021/ic5025668
Inorg. Chem. 2015, 54, 2160–2170

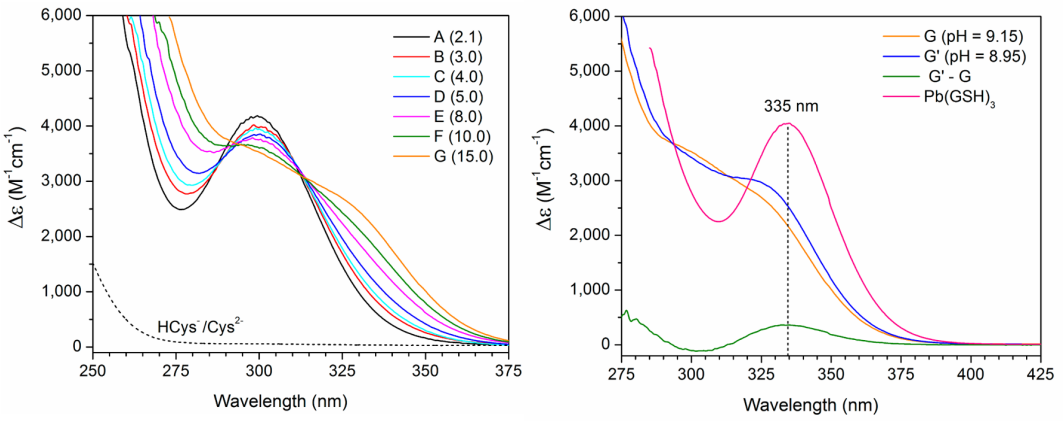

Figure 2. (left) UV−vis spectra of lead(II) cysteine solutions A−G with $C_{Pb^{II}}$ = 10 mM and H_2Cys/Pb^{II} mole ratios 2.1−15.0 compared with that of a 10 mM cysteine solution (dots, pH 9.1). (right) UV−vis spectra of 10 mM lead(II) solutions containing H_2Cys/Pb^{II} mole ratio 15.0 at pH 9.15 (solution G) and at pH 8.95 (solution G′) and their difference (G′ − G) compared with that of a lead(II) glutathione solution with GSH/Pb^{II} mole ratio 10.0 (pH 8.5).[33] Data interval = 0.5 nm.

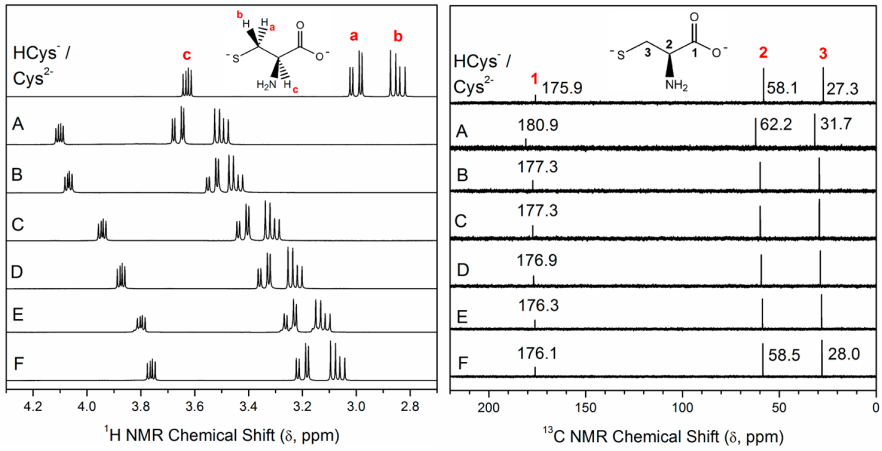

Figure 3. ^1H and ^{13}C NMR spectra of 0.1 M cysteine in D_2O (pH 9.1) and alkaline lead(II) cysteine solutions (99.9% D_2O) with $C_{Pb^{II}}$ = 10 mM and H_2Cys/Pb^{II} mole ratios 2.1 (A), 3.0 (B), 4.0 (C), 5.0 (D), 8.0 (E), and 10.0 (F). See Table 1.

amu in the spectrum of solution F. In negative-ion mode, only one mass peak corresponding to a lead(II) complex was observed, assigned to the $[Pb(H_2Cys)_2 - 3H^+]^-$ ion (446.99 amu).

Electronic Absorption Spectroscopy. Figure 2 (left) displays the UV−vis spectra for the lead(II) cysteine solutions A−G ($C_{Pb^{II}}$ = 10 mM). The absorption bands have been attributed to a combination of S^- 3p → Pb^{II} 6p ligand-to-metal charge-transfer and Pb^{II} intraatomic transitions.[37−40] The peak maximum for solution A, λ_{max} = 298 nm (C_{H_2Cys} = 21 mM; pH 10.4) shows a slight red shift to λ_{max} = 300 nm as the ligand concentration increases in solution B with H_2Cys/Pb^{II} mole ratio 3.0 at pH 9.1 (Figure S-4a in the SI).

For solutions E−G with high free ligand concentration (50−120 mM), a growing shoulder appears around $\lambda \sim 330$ nm, while the intensity of the peak at ~300 nm reduces significantly. This shoulder is blue-shifted relative to the maximum absorption recorded at 335 nm for a lead(II) glutathione solution (pH 8.5) containing excess ligand (Figure 2, right).[33] The amplitude of this shoulder is pH-dependent, as shown in Figure 2 (right) for 10 mM lead(II) solutions containing H_2Cys/Pb^{II} mole ratio 15.0 at pH 9.15 (solution G) and pH 8.95 (solution G′). The difference of these two spectra (G′ − G) shows that when the pH is lowered by 0.2 units, a peak at 335 nm emerges, very similar to λ_{max} in the UV−vis spectrum of the lead(II) glutathione solution.[33] There is no true isosbestic point around 312 nm, as shown in Figure S-4b in the SI by the systematic movement of crossing points of the absorption spectra of solutions B−G with that of solution A.

^1H and ^{13}C NMR Spectroscopy. The ^1H and ^{13}C NMR spectra of a 0.1 M cysteine solution (pH 9.1) and the lead(II) cysteine solutions A−F ($C_{Pb^{II}}$ = 10 mM) prepared in D_2O are shown in Figure 3, with the ^1H NMR chemical shifts (δ_H) shown in Table S-2 in the SI. For lead(II)-containing solutions, only one set of signals was observed for the H_a−H_c and C_1−C_3 atoms in both Pb^{II}-bound and free cysteine because of fast ligand exchange on the NMR time scale. These average resonances were all shifted downfield relative to the corresponding peaks in free cysteine (see Table S-2 in the SI), with the largest shifts ($\Delta\delta$) observed for solution A (H_2Cys/Pb^{II} mole ratio = 2.1), which contains the least amount of free ligand. Satellites originating from ^{207}Pb nuclei were not observed in the ^{13}C NMR spectra.

DOI: 10.1021/ic5025668
Inorg. Chem. 2015, 54, 2160−2170

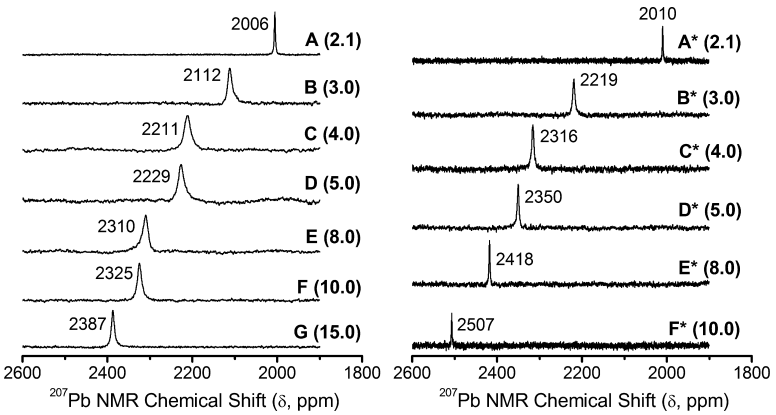

Figure 4. ^{207}Pb NMR spectra of the alkaline aqueous lead(II) cysteine solutions A−G enriched in ^{207}Pb ($C_{Pb^{II}}$ = 10 mM; H_2Cys/Pb^{2+} mole ratios 2.1−15.0) and A*−F* with 10% D_2O ($C_{Pb^{II}}$ = 100 mM; H_2Cys/Pb^{2+} mole ratios 2.1−10.0).

^{207}Pb NMR Spectroscopy. The chemical shift of the ^{207}Pb nucleus spans over a wide range (~17000 ppm). It is sensitive to the local structure and electronic environment, the nature of surrounding donor atoms, the bond covalency, and the coordination number and is affected by the temperature and concentration.[27,28,41−43] We measured ^{207}Pb NMR spectra for two sets of alkaline aqueous lead(II) cysteine solutions (containing 10% D_2O), with increasing H_2Cys/Pb^{II} mole ratios (Table 1). Calculated distribution diagrams based on different sets of stability constants indicate that the dominating lead(II) complexes would be either $[Pb(Cys)_2]^{2-}$ (Figure S-2b in the SI),[20] or a mixture of $[Pb(Cys)_2]^{2-}$ and $[Pb(Cys)(HCys)]^{-}$ (Figure S-1b in the SI).[16] Figure 4 presents the ^{207}Pb NMR spectra for solutions A−G ($C_{Pb^{II}}$ = 10 mM; enriched in ^{207}Pb) and A*−F* ($C_{Pb^{II}}$ = 100 mM), all with only an average NMR resonance. Solutions A and A*, both with the H_2Cys/Pb^{II} mole ratio = 2.1 at pH 10.4, show sharp signals at 2006 and 2010 ppm, respectively, which are ~184−200 ppm deshielded relative to that of lead(II) penicillamine (3,3′-dimethylcysteine) solutions with similar composition (~1806−1826 ppm).[26] The sharpness of this signal results from fast ligand exchange (in the NMR time scale) between the lead(II) complexes in solution. As the ligand concentration increases in solutions B and B* (H_2Cys/Pb^{II} = 3.0) and the pH changes to 9.1, the ^{207}Pb resonance becomes broader and shifts ~106 (B) and ~209 (B*) ppm downfield and more for the higher ligand concentration. Broad averaged signals indicate ligand exchange between several lead(II) species at intermediate rates. Solution F* containing $C_{Pb^{II}}$ = 100 mM and C_{H_2Cys} = 1.0 M shows the most deshielded ^{207}Pb NMR resonance (2507 ppm), which still is ~286 ppm upfield relative to that of the Pb(*S*-GSH)$_3$ complex (2793 ppm) with PbS_3 coordination.[33]

For comparison, we measured one-pulse MAS ^{207}Pb NMR spectra of the crystalline bis(2-aminoethanethiolato)lead(II) complex, Pb(*S*,*N*-aet)$_2$, at two different spin rates, 5.5 and 5.8 kHz (see Figures 5 and S-5a in the SI), and observed an isotropic chemical shift of δ_{iso} = 2105 ppm for this complex with PbS_2N_2 coordination.[25] Reconstruction of a static ^{207}Pb NMR powder pattern for spin rate 5.8 kHz resulted in the following principal components: δ_{11} = 3707.98 ppm, δ_{22} = 2831.04 ppm, δ_{33} = −223.12 ppm, leading to $\delta_{iso} = 1/3(\delta_{11} + \delta_{22} + \delta_{33})$ = 2105.3 ppm (see Figure S-5b in the SI). The isotropic chemical shift is ~600 ppm upfield relative to the only other ^{207}Pb chemical shift that is reported for PbS_2N_2 coordination, δ_{iso} = 2733 ppm for Pb(2,6-$Me_2C_6H_3S)_2(py)_2$ (py = pyridine). In that lead(II) complex, all ligands are monodentate (i.e., not forming a chelate ring) and pyridine is the N-donor ligand.[44]

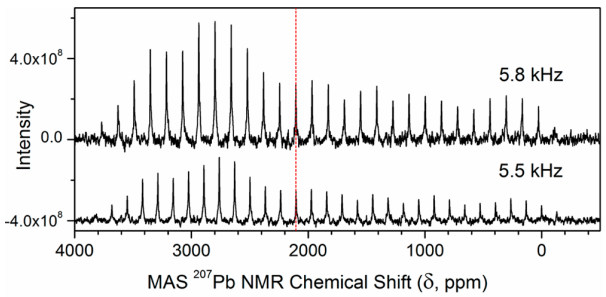

Figure 5. One-pulse proton-decoupled MAS ^{207}Pb NMR spectra of crystalline Pb(*S*,*N*-aet)$_2$, measured at two different spin rates (5.5 and 5.8 kHz) at room temperature. The dashed vertical line shows the isotropic chemical shift δ_{iso} = 2105 ppm (identified from overlapping spectra in Figure S-5a in the SI).

We also obtained the ^{207}Pb NMR spectrum of an aqueous lead(II) cysteamine solution, prepared by dissolving crystalline (mononuclear) Pb(aet)$_2$ in a solution containing the same number of moles of cysteamine, with a final lead(II)/cysteamine mole ratio of 1:3 (10% D_2O; $C_{Pb^{II}}$ ~ 76 mM; pH 10.1). A signal at 2212 ppm was observed (Figure S-6 in the SI), probably from a mixture of mononuclear Pb(*S*,*N*-aet)$_2$ (PbS_2N_2 coordination), $[Pb(S,N\text{-aet})(S\text{-Haet})(OH/OH_2)]^n$ (n = 0, 1; PbS_2NO), and $[Pb(S,N\text{-aet})(S\text{-Haet})_2]^+$ (PbS_3N) complexes. A minor amount of PbS_3N species is a likely reason for the ~100 ppm deshielding of the ^{207}Pb NMR resonance for this solution, relative to the isotropic chemical shift of crystalline Pb(aet)$_2$ (δ_{iso} = 2105 ppm). Moreover, multinuclear species such as the $[Pb_2(aet)_3]^+$ complex may form,[45] where Pb^{II} ions can adopt PbS_3N coordination through bridging thiolate groups. However, Li and Martell could only identify mononuclear $[Pb(Haet)]^{2+}$, $[Pb(aet)]^+$, and Pb(aet)-(OH) complexes in dilute solutions with $C_{Pb^{II}}$ = 1.0 mM (C_{Haet} = 1.0−2.0 mM; pH 2−8).[46]

Pb L_{III}-Edge XAS. The near-edge features in the XAS spectra are nearly identical for the lead(II) cysteine solutions, as shown in Figure S-7 in the SI, and are evidently not sensitive to the changes in lead(II) speciation as the ligand concentration

DOI: 10.1021/ic5025668
Inorg. Chem. 2015, 54, 2160−2170

DOCKET ALARM

Explore Litigation Insights

Docket Alarm provides insights to develop a more informed litigation strategy and the peace of mind of knowing you're on top of things.

Real-Time Litigation Alerts

Keep your litigation team up-to-date with **real-time alerts** and advanced team management tools built for the enterprise, all while greatly reducing PACER spend.

Our comprehensive service means we can handle Federal, State, and Administrative courts across the country.

Advanced Docket Research

With over 230 million records, Docket Alarm's cloud-native docket research platform finds what other services can't. Coverage includes Federal, State, plus PTAB, TTAB, ITC and NLRB decisions, all in one place.

Identify arguments that have been successful in the past with full text, pinpoint searching. Link to case law cited within any court document via Fastcase.

Analytics At Your Fingertips

Learn what happened the last time a particular judge, opposing counsel or company faced cases similar to yours.

Advanced out-of-the-box PTAB and TTAB analytics are always at your fingertips.

API

Docket Alarm offers a powerful API (application programming interface) to developers that want to integrate case filings into their apps.

LAW FIRMS
Build custom dashboards for your attorneys and clients with live data direct from the court.

Automate many repetitive legal tasks like conflict checks, document management, and marketing.

FINANCIAL INSTITUTIONS
Litigation and bankruptcy checks for companies and debtors.

E-DISCOVERY AND LEGAL VENDORS
Sync your system to PACER to automate legal marketing.